

Article

A search for a spectral technique to solve nonlinear fractional differential equations

Malgorzata Turalska ^{1,†*} and Bruce J. West ^{1,2,†}¹ Department of Physics, Duke University, Durham, NC 27709, USA² Information Science Directorate, US Army Research Office, Research Triangle Park, NC 27708, USA

† These authors contributed equally to this work.

* Author to whom correspondence should be addressed; mat51@phy.duke.edu, 9196602582

Version August 14, 2015 submitted to Entropy. Typeset by L^AT_EX using class file mdpi.cls

Abstract: A spectral decomposition method is used to obtain solutions to a class of nonlinear differential equations. We extend this approach to the analysis of the fractional form of these equations and demonstrate the method by applying it to the fractional Riccati equation, the fractional logistic equation and a fractional cubic equation. The solutions reduce to those of the ordinary nonlinear differential equations, when the order of the fractional derivative is $\alpha = 1$. The exact analytic solutions to the fractional nonlinear differential equations are not known, so we evaluate how well the derived solutions satisfy the corresponding fractional dynamic equations. In the three cases we find a small, apparently generic, systematic error that we are not able to fully interpret.

Keywords: fractional calculus; nonlinear fractional differential equations; spectral decomposition; operators; eigenvalues

1. Introduction

Herein we propose a spectral method for solving fractional nonlinear rate equations of a certain kind. The method is not perturbative, but neither is it exact, since it gives rise to systematic deviations of the analytic solution from the numerical solution at intermediate times that reaches a maximum value of 2%. On the one hand, the spectral method provides a remarkable good approximation to numerical calculation. On the other hand, the source of the small but systematic deviation from the numerical solution remains a mystery. This paper presents the approach in detail and introduces a new problem that requires explanation.

20 Despite the advances made into the understanding of complex nonlinear systems in the last half of the
21 twentieth century, many physical phenomena failed to be described using the tools of ordinary calculus.
22 Nonlocal distributed effects and memory effects observed in relaxation phenomena [1], living systems [2,
23 3], wave propagation in porous materials [4] have been more successfully modeled within the framework
24 of the fractional calculus [5]. Fractional differential equations (FDE) have been adopted to explain these
25 and other complex phenomena [6,7]. Since exact solutions to the majority of FDEs are not available,
26 the search for appropriate analytical and numerical methods is a subject of ongoing research. Recently,
27 a number of approaches devoted to solving FDEs have been proposed. Examples include Adomian
28 decomposition method [8], homotopy perturbation method [9,10], the fractional sub-equation method,
29 and the Haar wavelet method [11], to name but a few. However, the convergence region of solutions
30 obtained with these algorithms is rather small.

31 It was hypothesized [12] that the spectral decomposition method can be extended to the analysis
32 of a class of nonlinear fractional differential equations (NFDEs). Herein we demonstrate the method
33 by applying it to the fractional Riccati equation (FRE), the fractional logistic equation (FLE) and a
34 fractional cubic equation (FCE), where the fractional-order is in the range $0 < \alpha \leq 1$. The solutions
35 obtained are shown to have the correct short-time and long-time behaviors. Additionally, they reduce to
36 the well known solutions of the ordinary nonlinear differential equations, when the order of the fractional
37 derivative is $\alpha = 1$. In the cases considered herein the exact analytic solution to the NFDE was not
38 known previously, we evaluate how well the derived solutions satisfy the corresponding NFDE using
39 numerical techniques. In all cases we find a very small, but systematic deviation of the analytic from the
40 numerical solutions that has eluded our best efforts to interpret. One possibility, of course, is that the
41 numerical technique used to solve the NFDE is the culprit, since it was based on numerically solving
42 linear fractional equations. But this remains to be investigated.

43 In Section 2 we introduce the spectral decomposition of the solution to define the eigenvalue problem
44 for integer-order linear and nonlinear rate equations, as well as NFDEs. In Section 3 we obtain a
45 series expansion over the spectrum of eigenvalues and eigenfunctions for the solution to three NFDEs,
46 where the exponentials in the solutions to the integer-order equations, also obtained, are replaced with
47 Mittag-Leffler functions (MLFs). Exact solutions to NFDEs are rare in the literature [13,14], so to test the
48 validity of the analytic results we numerically evaluate how the solutions obtained satisfy the appropriate
49 NFDE. To our surprise the error function measuring this fit is not zero, but varies in time, increasing as
50 $t^{2\alpha}$ at early times and decreasing as $t^{-\alpha}$ at late times, and reaching a maximum difference of less than a
51 few percent at an intermediate time. This non-monotonic scaling difference is shown to occur with the
52 solutions to the FRE, the FLE, as well as, the FCE, all with the same qualitative behavior in the error.
53 In Section 8 we draw some tentative conclusions including the speculation that this systematic deviation
54 may be generic.

55 2. Spectral decomposition

56 2.1. Integer operator

Let us begin by establishing the nomenclature used in the study of the nonlinear differential equations. Consider the one-dimensional first-order differential equation

$$\frac{d}{dt}X(t) = \mathcal{O}X(t), \quad (1)$$

where $X(t)$ is the dynamic variable of interest and \mathcal{O} is a generic operator acting on $X(t)$. Allowing Eq. (1) to describe any dynamical system of interest entails the formal solution

$$X(t) = e^{\mathcal{O}_0 t} x_0, \quad (2)$$

where $x_0 \equiv X(0)$ defines the initial condition in the phase space for the dynamic variable and the operator \mathcal{O}_0 acts on the initial condition. The exponential operator is formally defined by the series expansion

$$e^{\mathcal{O}_0 t} = \sum_{k=0}^{\infty} \frac{(\mathcal{O}_0 t)^k}{\Gamma(k+1)} \quad (3)$$

so that the solution Eq.(2) can be expressed as

$$X(t) = \sum_{k=0}^{\infty} \frac{(\mathcal{O}_0 t)^k}{\Gamma(k+1)} x_0 = \sum_{k=0}^{\infty} \frac{t^k}{\Gamma(k+1)} \mathcal{O}_0^k x_0 \quad (4)$$

where the operator \mathcal{O}_0^k acts solely on the initial condition. Note that for a linear equation with a constant rate λ the operator is given by

$$\mathcal{O}_0^k x_0 = \left(\lambda x_0 \frac{\partial}{\partial x_0} \right)^k x_0 = \lambda^k x_0, \quad (5)$$

which when inserted into Eq.(4) and summing the series yields the exponential solution to the scalar rate equation

$$X(t) = e^{\lambda t} x_0. \quad (6)$$

It is apparent that Eq.(5) has a form suggestive of an eigenvalue equation and that the solution to the general integer-operator rate equation can be expressed as an eigenfunction expansion over the spectrum of eigenvalues

$$X(t) = \sum_{k=0}^{\infty} C_k \phi_k(x_0) \chi_k(t). \quad (7)$$

The quantity $\phi_k(x_0) \chi_k(t)$ is the eigenfunction, factored into a piece determined by the spectrum of eigenvalues $\{\lambda_k; k = 0, 1, 2, \dots\}$, a piece determined by the initial condition x_0 , and the expansion coefficient C_k determined by the dynamics and overall initial normalization. Inserting Eq.(7) into (1), allows us to separate out the time-dependence of the components of the expansion

$$\frac{d}{dt} \chi_k(t) = \lambda_k \chi_k(t) \Rightarrow \chi_k(t) = e^{\lambda_k t}. \quad (8)$$

Correspondingly, the eigenvalue equations are given by

$$\mathcal{O}_0 \phi_k(x_0) = \lambda_k \phi_k(x_0) \quad (9)$$

57 and the eigenvalues are determined by the form of the operator.

In the linear case just considered the operator is the same as before, so the equation for the eigenfunction is

$$\lambda x_0 \frac{d\phi_k}{dx_0} = \lambda_k \phi_k$$

with the solution

$$\phi_k(x_0) = x_0^{\frac{\lambda_k}{\lambda}}.$$

The linear eigenvalue spectrum is degenerate $\lambda_k = \lambda$ and the coefficients are determined from the initial condition to satisfy

$$\sum_{k=0}^{\infty} C_k = 1.$$

58 The resulting solution is, of course, given by Eq.(6).

59 2.2. Non-integer (fractional) operator

Now assume that this general form of a solution to a differential equation translates to the fractional calculus domain. Thus, we replace Eq.(1) with the fractional differential equation

$$\frac{d^\alpha}{dt^\alpha} X(t) = \mathcal{O}X(t), \quad (10)$$

where $0 < \alpha \leq 1$. We assume the fractional derivative to be defined in the Caputo sense:

$$\frac{d^\alpha}{dt^\alpha} X(t) = \frac{1}{\Gamma(1-\alpha)} \int_0^t \frac{X'(\tau)}{(t-\tau)^\alpha} d\tau. \quad (11)$$

where $X'(\tau)$ denotes the derivative of $X(\tau)$ with respect to its argument. Eq.(10) can be solved analytically in terms of the MLF by employing the spectral decomposition introduced above in which case we have for the components of the eigenfunction

$$\frac{d^\alpha}{dt^\alpha} \chi_k(t) = \lambda_k \chi_k(t), \quad (12)$$

to obtain the MLF evaluated over the spectrum of eigenvalues

$$\chi_k(t) = E_\alpha(\lambda_k t^\alpha). \quad (13)$$

The MLF is defined by the series [15,16]

$$E_\alpha(z) = \sum_{k=0}^{\infty} \frac{z^k}{\Gamma(k\alpha + 1)}. \quad (14)$$

Consequently, inserting the MLF into the expansion for the solution yields [12]

$$X(t) = \sum_{k=0}^{\infty} C_k \phi_k(x_0) E_\alpha(\lambda_k t^\alpha) \quad (15)$$

60 and the eigenvalues are determined by the operator in Eq.(9). The MLF reduces to an exponential
61 function when $\alpha = 1$, reducing the series expansion to the ordinary solution of Eq.(2) in that case.

62 Note that we can adopt the same formal spectral decomposition employed for the integer-derivative
63 case discussed above for the fractional-order dynamics considered here. But, before we explore the
64 fractional case, let us examine an integer-order nonlinear dynamic equation.

65 3. Riccati equation

We illustrate the spectral decomposition method, applied to a nonlinear rate equation, using the reduced form of the Riccati equation [17]:

$$\frac{d}{dt}X(t) = 1 - X^2(t) = \mathcal{O}X(t). \quad (16)$$

The Riccati equation is put into the form of Eq.(1) by introducing the phase space operator \mathcal{O} :

$$\mathcal{O} = (1 - x^2) \frac{\partial}{\partial x}, \quad (17)$$

and the formal solution to the Riccati equation can be written as the eigenmode expansion

$$X(t) = \sum_{k=0}^{\infty} C_k \phi_k(x_0) e^{\lambda_k t}. \quad (18)$$

66 The dependence of the solution on the initial condition can be described by the eigenfunctions equation

$$\begin{aligned} \mathcal{O}_0 \phi_k(x_0) &\equiv [1 - x_0^2] \frac{d\phi_k(x_0)}{dx_0} \\ &= \lambda_k \phi_k(x_0). \end{aligned} \quad (19)$$

The solution to Eq.(19) is given by

$$\ln \phi_k(x_0) = \frac{\lambda_k}{2} \ln \left[\frac{1 + x_0}{1 - x_0} \right],$$

67 where we need to determine the spectrum of eigenvalues $\{\lambda_k\}$.

This last expression is inserted into Eq. (18) to obtain

$$X(t) = \sum_{k=0}^{\infty} C_k \left[\frac{1 + x_0}{1 - x_0} \right]^{\frac{\lambda_k}{2}} e^{\lambda_k t}. \quad (20)$$

It is straightforward to obtain the eigenvalues $\lambda_k = -2k$ by inserting Eq.(20) into Eq.(16) and equating coefficients of time dependent terms, as well as the coefficients for equal k values

$$C_k = 2 \left(\frac{C_1}{2} \right)^k ; k > 0.$$

The series solution is then

$$X(t) = 2 \sum_{k=0}^{\infty} \left(\frac{C_1}{2} \right)^k \left(\frac{1 - x_0}{1 + x_0} \right)^k e^{-2kt}.$$

The final expansion coefficient is determined to be $C_1 = -2$ from the initial condition, so that the solution to the nonlinear initial value problem becomes

$$X(t) = 2 \sum_{k=0}^{\infty} \left(\frac{x_0 - 1}{x_0 + 1} \right)^k e^{-2kt} - 1 \quad (21)$$

Additionally, for $x_0 = 0$, Eq.(21) reduces to the well-known solution of Riccati equation [17]

$$X(t) = \tanh(t).$$

For initial values $x_0 \neq 0$ the solution to Eq. (16) is obtained by summing the series in Eq.(21) to obtain

$$X(t) = \frac{\tanh(t) + x_0}{x_0 \tanh(t) + 1} \quad (22)$$

68 also in agreement with the solution obtain by Davis [17].

Since we have an exact solution we can test the series expansion computationally. The error is defined as the difference between the time derivative of the series solution obtained using Eq.(21) and the known exact solution given by Eq.(22) inserted into the right hand side of the Riccati equation:

$$\Delta(t) = 2 \sum_{k=0}^{\infty} \left(\frac{x_0 - 1}{x_0 + 1} \right)^k (-2k) e^{-2kt} - 1 + \left[\frac{\tanh(t) + x_0}{x_0 \tanh(t) + 1} \right]^2. \quad (23)$$

69 The sum is estimated by its first 100 terms yielding a difference on the order of 10^{-15} , which matches
70 machine precision, affirming that the series given by Eq. (21) is a valid solution to the Riccati equation.

71 4. Fractional Riccati equation

72 4.1. Spectral decomposition solution

We now establish that a generalization of the spectral decomposition method leads to valid solutions for certain NFDEs. We start from the fractional form of the Riccati equation

$$\frac{d^\alpha}{dt^\alpha} X(t) = 1 - X^2(t) = \mathcal{O}X(t) \quad (24)$$

where $0 < \alpha < 1$. If the fractional derivative is of the Caputo type, Eq.(24) has the operator given by Eq.(17). Consequently, the solution to the FRE is of the form

$$X(t) = \text{sum}_{k=0}^{\infty} C_k \phi_k(x_0) E_\alpha(\lambda_k t), \quad (25)$$

and the eigenvalue problem is the same as for the integer-order Riccati equation, that is, given by Eq.(19). Consequently, we have the same spectrum of eigenvalues obtained in the integer-order RE, obtained at early times using the stretched form of the MLF. In the same way the expansion coefficients are the same as previously obtained in order to satisfy the initial condition and we obtain for the solution to the FRE:

$$X(t) = 2 \sum_{k=0}^{\infty} \left(\frac{x_0 - 1}{x_0 + 1} \right)^k E_\alpha(-2kt^\alpha) - 1. \quad (26)$$

We note that the solution obtained to the FRE does not coincide with that obtained by Zhang *et al.* [14]. However we point out that these authors use Jumarie's modified form of the Reimann-Liouville fractional derivative [18], which explicitly satisfies the Leibniz condition:

$$\frac{d^\alpha}{dt^\alpha} [f(t)g(t)] = g(t) \frac{d^\alpha f(t)}{dt^\alpha} + f(t) \frac{d^\alpha g(t)}{dt^\alpha}$$

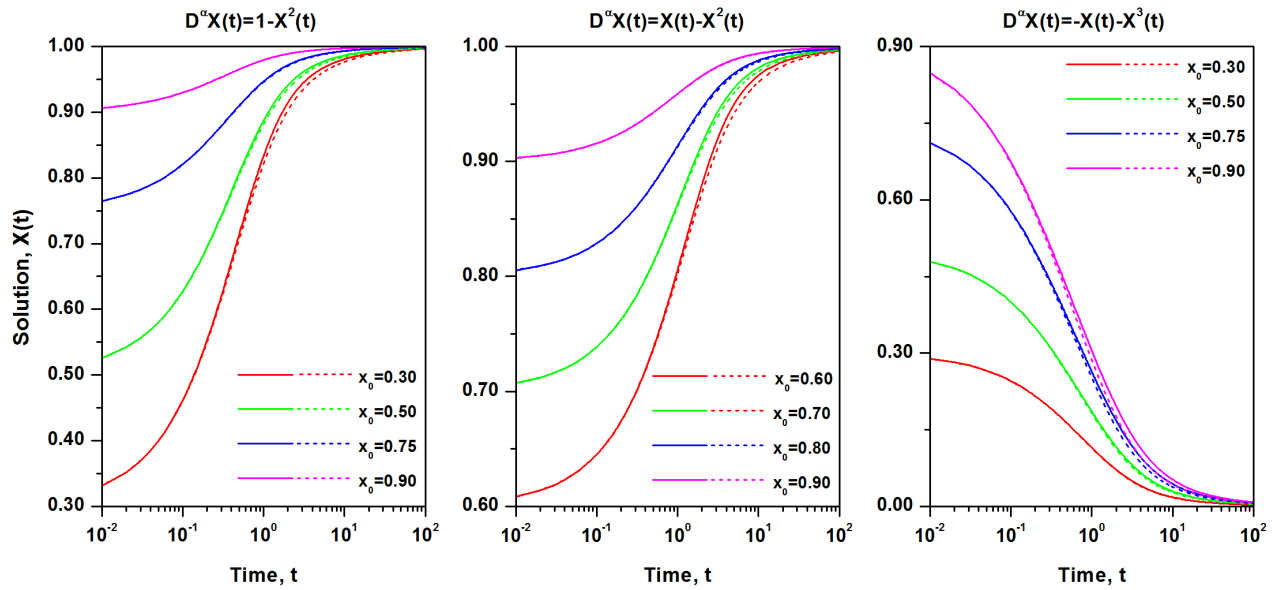


Figure 1. Solutions to the fractional differential equations. (*left*) Fractional Riccati differential equation, as defined by Eq. 26. (*middle*) Fractional logistic equation, as defined by Eq. 37. The growth rate is $\lambda = 1.00$. (*right*) The cubic fractional equation, as defined by Eq. 48, with $a = b = 1.00$. The order of the fractional derivative in all cases is $\alpha = 0.75$. Continuous lines correspond to solutions obtained with the spectral decomposition method, dashed lines correspond to numerical integration of given equations. The integration step is $h = 10^{-3}$.

73 for the derivative of the product of two analytic functions $f(t)$ and $g(t)$. It is evident that the Caputo
 74 fractional derivative does not satisfy the Leibniz condition [15,16] and consequently, although the
 75 starting dynamic equations look the same, that because of the restrictions on the fractional derivatives,
 76 the problem solved by Zhang et al. [14] is different from the FRE considered here.

77 We see in this figure that the analytic solution does extremely well in following the numerical solution
 78 to the FRE, but it is not exact. The numerical solutions for various initial conditions, obtained using
 79 Eq.(26), where the infinite sum is approximated by its first 100 elements, are demonstrated in the first
 80 panel of the tryptic in Figure 1. One can easily verify that the proposed solution satisfies the initial
 81 condition and has the correct long time behavior. But since there are no known exact solutions to the
 82 initial value problem for the NRE, we use the numerical test introduced previously to test the veracity of
 83 Eq.(26).

84 4.2. Testing the solution

Since the exact analytic solution to the FRE Eq. (24) is not known, one possible approach to check the
 validity of Eq.(26) is to check that this solution satisfies the fractional differential equation in question.
 Applying the Caputo definition of fractional derivative to the analytic solution to the RME yields

$$LHS = \frac{d^\alpha}{dt^\alpha} X(t) = 2 \sum_{k=0}^{\infty} \left(\frac{x_0 - 1}{x_0 + 1} \right)^k (-2k) E_\alpha(-2kt^\alpha), \quad (27)$$

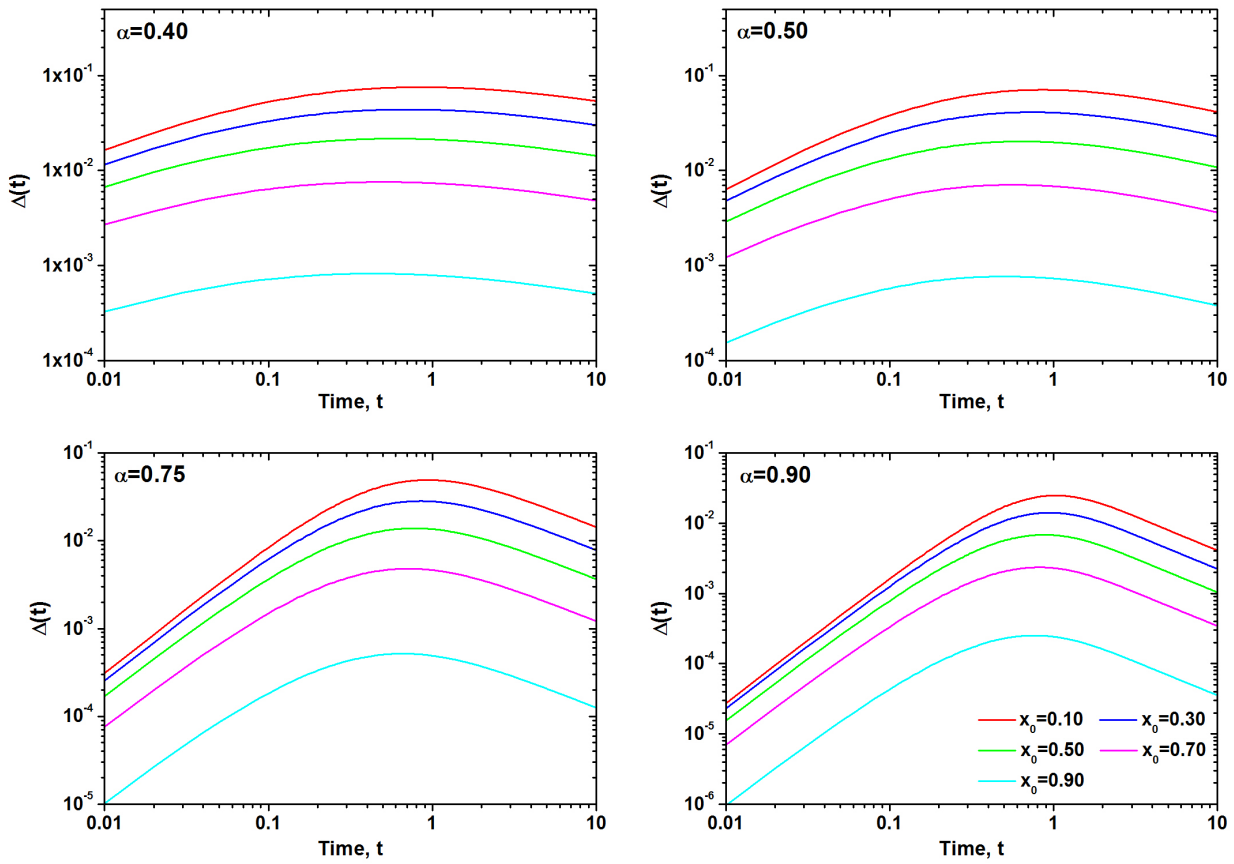


Figure 2. The difference $\Delta(t)$ between the RHS and LHS of the fractional Riccati equation, when the solution is assumed to be Eq. 26. Consecutive panels correspond to an increasing order of the fractional derivative α . Color lines correspond to range of initial conditions, as denoted by the legend in lower right plot.

while the right hand side of the FRE is

$$RHS = 1 - X^2(t) = 1 - \left(2 \sum_{k=0}^{\infty} \left(\frac{x_0 - 1}{x_0 + 1} \right)^k E_{\alpha}(-2kt^{\alpha}) - 1 \right)^2. \quad (28)$$

Again the potential error is defined in terms of the difference

$$\Delta(t) = RHS - LHS, \quad (29)$$

which for an exact solution should be zero. This error variable is estimated numerically, and its behavior is plotted in Figure 2 for four values of α . It is apparent that the difference variable $\Delta(t)$ departs from zero at early times, gradually increasing, reaching a maximum value at $t \approx 1$, and finally decreases at long times. The behavior of $\Delta(t)$ and its maximum value $\Delta_{\max} < \text{a few percent}$, clearly depends on the order of the fractional derivative, α , and on the initial condition x_0 . The precise form of power-law scaling of $\Delta(t)$, present at short and long times, is obtained adopting an approximation to the MLF. At early times, the series defining the MLF (Eq. 14) reduces to a stretched exponential function

$$E_{\alpha}^0 = \lim_{t \rightarrow 0} E_{\alpha}(-\lambda t^{\alpha}) = 1 - \frac{\lambda t^{\alpha}}{\Gamma(1 + \alpha)} + \dots = \exp \left[-\frac{\lambda t^{\alpha}}{\Gamma(1 + \alpha)} \right], \quad (30)$$

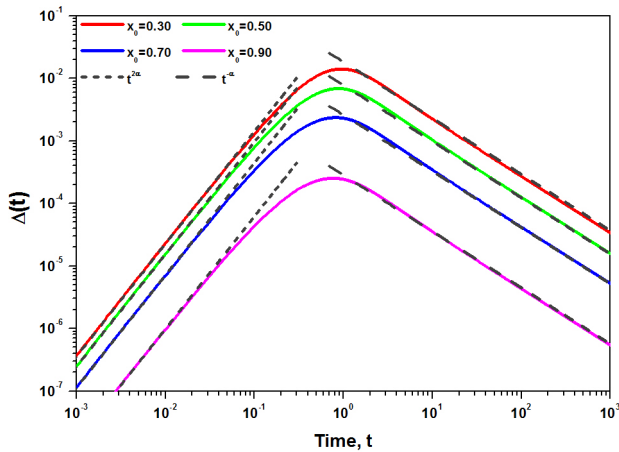


Figure 3. Short and long time power law behavior of the error function $\Delta(t)$. Both regimes are approximated by equations 32 and 33, respectively. The order of the fractional derivative $\alpha = 0.90$.

while at late times the MLF has inverse-power law behavior

$$E_{\alpha}^{\infty} = \lim_{t \rightarrow \infty} E_{\alpha}(-\lambda t^{\alpha}) = \frac{t^{-\alpha}}{\lambda \Gamma(1 - \alpha)}. \quad (31)$$

Thus, at early times the difference $\Delta(t)$ scales as $t^{2\alpha}$ and after some algebra this difference is determined to be

$$\Delta^0(t) = \lim_{t \rightarrow 0} \Delta(t) = \frac{t^{2\alpha}}{\Gamma^2(1 + \alpha)} (1 - x_0^2)^2, \quad (32)$$

while the long-time behavior of the difference is determined by direct calculation to scale as $t^{-\alpha}$:

$$\Delta^{\infty}(t) = \lim_{t \rightarrow \infty} \Delta(t) = \frac{t^{-\alpha}}{\Gamma(1 - \alpha)} \left[2 \log \left(\frac{x_0 + 1}{2} \right) + x_0 + 1 - \frac{\log^2 \left(\frac{x_0 + 1}{2} \right)}{\Gamma(1 - \alpha)} t^{-\alpha} \right] \quad (33)$$

85 Figure 3 illustrates the validity of both approximations to the difference $\Delta(t)$ for selected orders of the
 86 fractional derivative. It is evident that the deviation of the solution obtained by spectral decomposition
 87 deviates from the exact solution in systematic ways at both late and early times. The maximum difference
 88 for $\alpha = 0.9$ is shown in this figure to be below 2%, but the explanation as to why the deviation behaves
 89 the way it does remains elusive. Therefore we examine the solutions obtained by applying the technique
 90 to two other well known nonlinear initial value problems extended to the fractional domain.

91 5. Fractional logistic equation

92 5.1. Spectral decomposition solution

Next we examine the fractional logistic equation (FLE)

$$\frac{d^{\alpha}}{dt^{\alpha}} X(t) = \lambda^{\alpha} X(t) (1 - X(t)) \quad (34)$$

where $X(t)$ is the normalized population and λ is the population growth rate. As before we define a phase space operator

$$\mathcal{O} = \lambda^\alpha x(1-x) \frac{\partial}{\partial x} \quad (35)$$

93 and write the formal solution as Eq.(25). The eigenvalue equation is slightly different from that for the
94 FRE

$$\begin{aligned} \mathcal{O}_0 \phi_k(x_0) &= \lambda^\alpha x_0(1-x_0) \frac{d\phi_k(x_0)}{dx_0} \\ &= \lambda_k \phi_k(x_0) \end{aligned} \quad (36)$$

After some algebra we obtain for the eigenfunctions

$$\phi_k(x_0) = \left(\frac{x_0}{1-x_0} \right)^{\frac{\lambda_k}{\lambda^\alpha}}$$

and after some algebra, using the spectral decomposition method, we arrive at the eigenvalues $\lambda_k = -k\lambda^\alpha$, the expansion coefficients $C_k = C_1^k$ and from the initial condition $C_1 = -1$. Inserting these quantities into the formal solution Eq.(25) yields

$$X(t) = \sum_{k=0}^{\infty} \left(\frac{x_0-1}{x_0} \right)^k E_\alpha(-k\lambda^\alpha t^\alpha). \quad (37)$$

95 where again x_0 is the initial condition. The numerical solutions for various initial conditions, obtained
96 using Eq.(37), where the infinite sum is approximated by its first 100 elements, are demonstrated in the
97 middle panel of the tryptic in Figure 1. As you might expect the solutions are qualitatively the same as
98 in the first panel.

When $\alpha = 1$, Eq.(37) reduces to the well-known solution to the logistic equation

$$X(t) = \frac{x_0}{x_0 + (1-x_0)e^{-\lambda t}}, \quad (38)$$

99 yielding sigmoidal population growth from the initial value $X(0) = x_0$ to the saturation level $X(\infty) = 1$.

100 Note that even though the FRE and the FLE have quadratic nonlinearities, the spectra in the two case
101 are different. The former increasing as $2k$ and the latter as k , which also determines the difference in the
102 normalization parameter C_1 in the two cases.

103 The solution, given by Eq.(37), is identical to the one obtained by one of the authors [13] using the
104 Carleman embedding technique. The Carleman embedding approach has successfully determined the
105 solution to many nonlinear differential equations as presented and discussed by Kowalski and Steeb
106 [19]. The technique was applied to a FNDE in [13] to obtain an infinite-order hierarchy of fractional
107 moment equations, using Laplace transforms and solved using a matrix diagonalization method. A
108 modest deviation of the analytic solution from the numerical integration of the FLE was noted in this
109 earlier analysis.

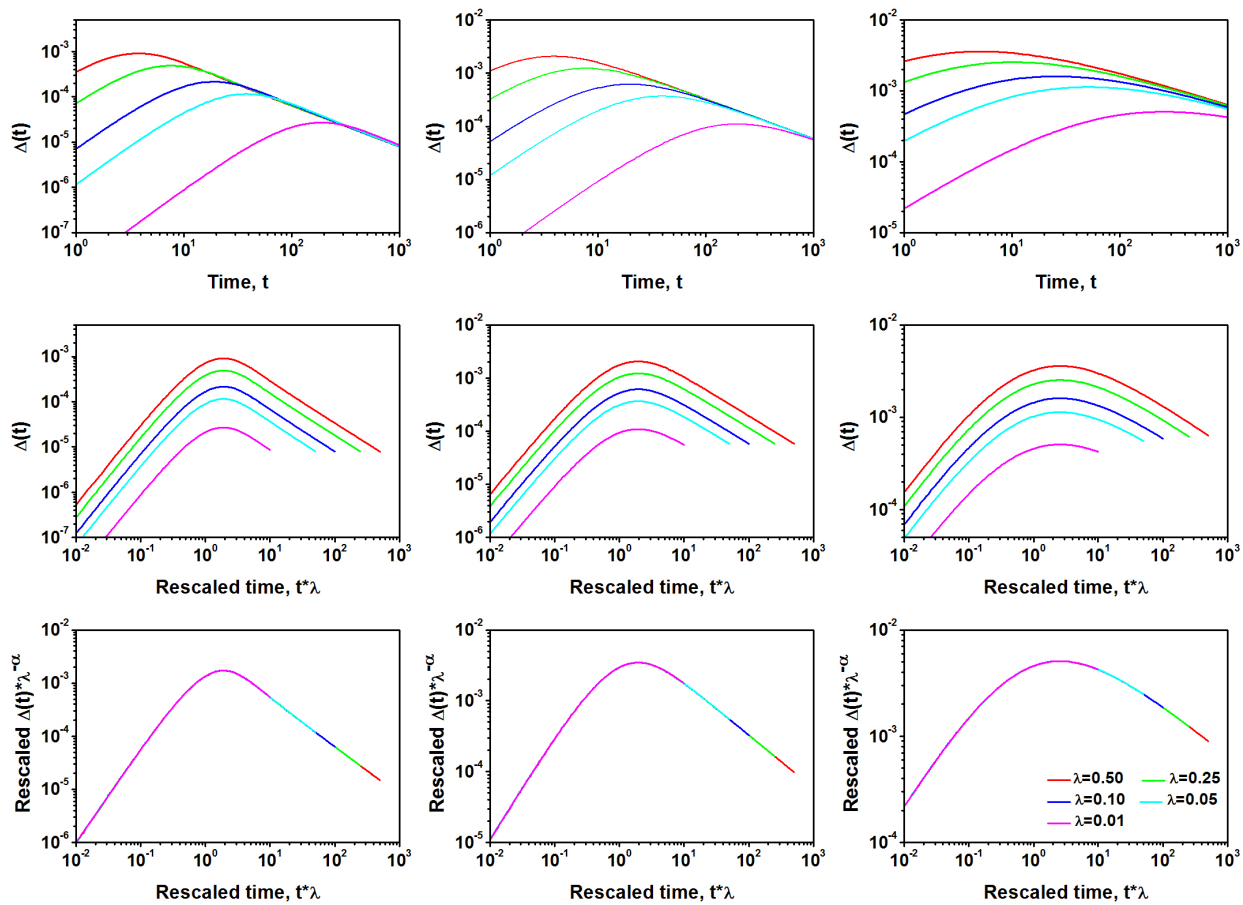


Figure 4. The difference $\Delta(t)$ between the RHS and LHS of the fractional logistic equation, when the solution is assumed to be Eq. 37. Columns correspond to decreasing values of α : $\alpha = 0.90$ (left), $\alpha = 0.75$ (middle) and $\alpha = 0.50$ (right). The initial value $x_0 = 0.75$ in all cases. Top row demonstrates the error function $\Delta(t)$ for a range of growth rate λ values. Middle row demonstrates the effect of rescaling time, while bottom row achieves complete overlap of $\Delta(t)$ curves generated for different λ through rescaling y -axis variable.

110 5.2. Testing the solution

Here again we check if the solution given by Eq.(37) satisfies the FLE by examining the difference equation. The left hand side of Eq.(34) is

$$LHS = \frac{d^\alpha}{dt^\alpha} X(t) = \sum_{k=0}^{\infty} \left(\frac{x_0 - 1}{x_0} \right)^k (-k\lambda^\alpha) E_\alpha(-k\lambda^\alpha t^\alpha), \quad (39)$$

111 while the right hand side is

$$RHS = \lambda^\alpha X(t) (1 - X(t)) \quad (40)$$

$$= \lambda^\alpha \sum_{k=0}^{\infty} \left(\frac{x_0 - 1}{x_0} \right)^k E_\alpha(-k\lambda^\alpha t^\alpha) \left(1 - \sum_{k'=0}^{\infty} \left(\frac{x_0 - 1}{x_0} \right)^{k'} E_\alpha(-k'\lambda^\alpha t^\alpha) \right). \quad (41)$$

112 The difference or potential error is defined as before by Eq.(29).

113 Figure 4 demonstrates the behavior of $\Delta(t)$ for selected values of the order of the fractional derivative
114 α , the initial condition x_0 and the unperturbed growth rate λ . We observe the same dependence of the

115 difference $\Delta(t)$ on time as in the case of the FRE. Note again that the the difference is not monotonic,
 116 but has a maximum value of less than 1%, depending on α and x_0 . The location of maximum in time is
 117 a function of λ . Rescaling both the x -axis and y -axis as follows

$$t \rightarrow t\lambda \quad (42)$$

$$\Delta(t) \rightarrow \Delta(t)\lambda^{-\alpha} \quad (43)$$

118 normalizes the $\Delta(t)$ curves, making them independent of the growth rate, as shown by the bottom row
 119 of curves in the figure.

Adopting the short-time and long-time approximations to the MLF we find that at early times the difference $\Delta(t)$ scales as $t^{2\alpha}$:

$$\Delta^0(t) = \lim_{t \rightarrow 0} \Delta(t) = \frac{t^{2\alpha}}{\Gamma^2(1 + \alpha)} x_0^2 (x_0 - 1)^2, \quad (44)$$

while the long time behavior scales as $t^{-\alpha}$:

$$\Delta^\infty(t) = \lim_{t \rightarrow \infty} \Delta(t) = \frac{t^{-\alpha}}{\Gamma(1 - \alpha)} \left[(x_0 - 1 - \log x_0) - \frac{\log^2 x_0}{\Gamma(1 - \alpha)} t^{-\alpha} \right]. \quad (45)$$

120 The accuracy of the algebraically determined scaling is numerically demonstrated in Figure 5. Here
 121 again, the deviation of the solution determined using the spectral decomposition technique to solve the
 122 FLE from the exact numerical solution, is non-monotonic and never exceeds 1%. Thus, the worst case
 123 using this technique is better than the best obtained using many approximation techniques.

124 6. Cubic fractional differential equation

125 6.1. Spectral decomposition solution

The final equation that we consider is a fractional differential equation with a cubic term (FCE)

$$\frac{d^\alpha}{dt^\alpha} X(t) = -aX(t) - bX^3(t) = \mathcal{O}X(t). \quad (46)$$

126 The formal solution given by the spectral decomposition requires the solution to the eigenvalue equation

$$\begin{aligned} \mathcal{O}_0 \phi_k(x_0) &= -x_0 [a + bx_0^2] \frac{d\phi_k(x_0)}{dx_0} \\ &= \lambda_k \phi_k(x_0). \end{aligned} \quad (47)$$

The algebra providing the solution to the eigenvalue problem will be presented elsewhere. Here we record that the solution is given by sum over the eigenvalue spectrum

$$X(t) = \sum_{k=0}^{\infty} \frac{(2k-1)!!}{(2k)!!} \left(\frac{\frac{b}{a}x_0^2}{\frac{b}{a}x_0^2 + 1} \right)^k \frac{x_0}{\sqrt{\frac{b}{a}x_0^2 + 1}} E_\alpha(-(2k+1)at^\alpha), \quad (48)$$

127 where we have adopted the notation of double factorial $(2k)!! = 2k(2k-2)(2k-4)\dots$. The solutions
 128 obtained using Eq. (48) are presented on the right panel of Fig. 1.

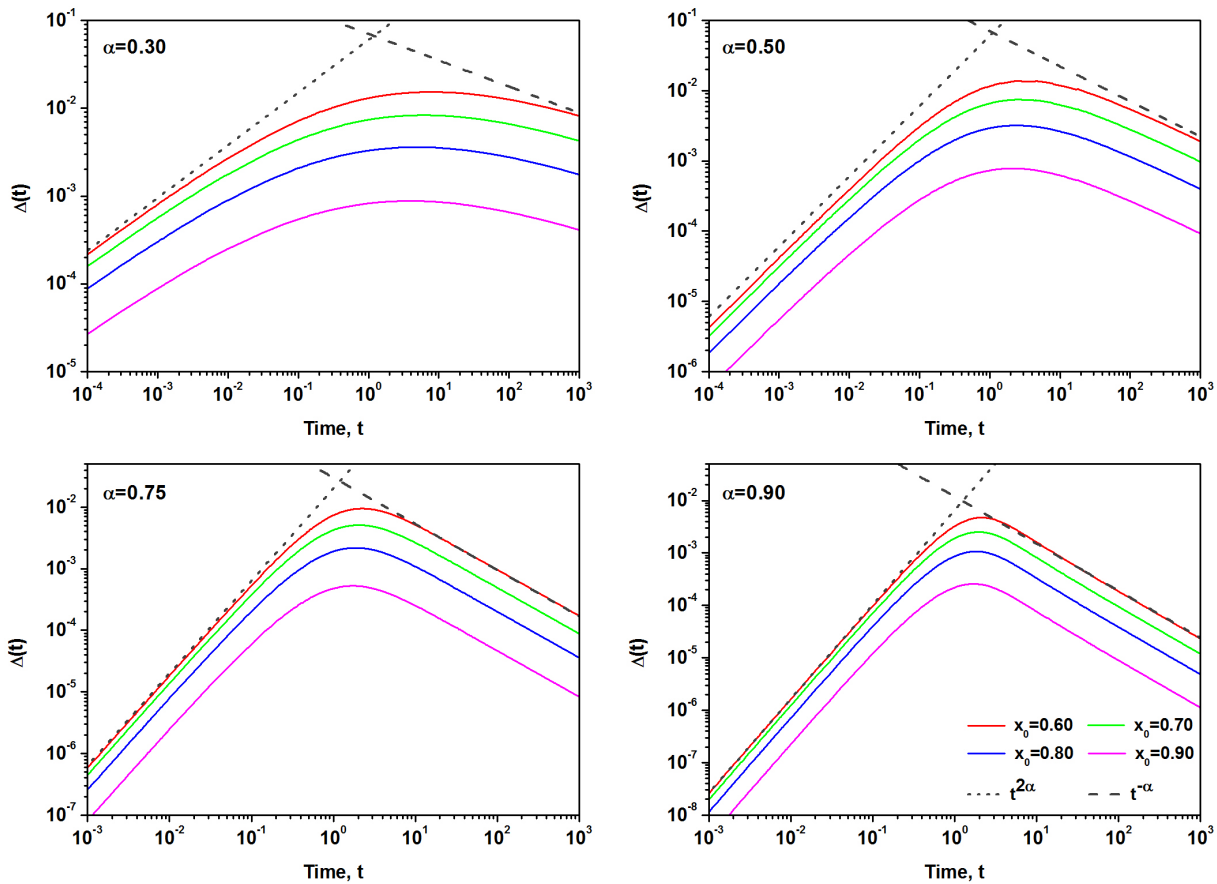


Figure 5. The difference $\Delta(t)$ between the RHS and LHS of the FLE. Consecutive panels correspond to an increasing order of the fractional derivative α . Color lines correspond to a range of initial conditions, as denoted by the legend in lower right plot. The growth rate in all cases is $\lambda = 1$.

For the integer-value case $\alpha = 1$, the MLF can again be replaced by an exponential in Eq.(48) and the series summed to yield the exact integer-value solution

$$X(t) = \frac{x_0 e^{-at}}{\sqrt{1 + \frac{b}{a} x_0^2 (1 - e^{-2at})}}. \quad (49)$$

129 6.2. Testing the solution

Once again we check how well this solution satisfies the NFDE in question by taking the difference between the two sides of the FCE. The difference or potential error function $\Delta(t)$ is illustrated on Figure 6 for $a = b = 1$. The short-time behavior of $\Delta(t)$ is

$$\Delta^0(t) = \lim_{t \rightarrow 0} \Delta(t) = \frac{t^{2\alpha}}{\Gamma^2(1 + \alpha)} x_0^3 (x_0 - 1)^2 \left[3 - \frac{t^\alpha}{\Gamma(1 + \alpha)} (x_0 - 1)^3 \right], \quad (50)$$

while the long-time behavior is

$$\Delta^\infty(t) = \lim_{t \rightarrow \infty} \Delta(t) = C_1(\alpha, x_0) \frac{t^{-\alpha}}{\Gamma(1 - \alpha)} + C_2(\alpha, x_0) \frac{t^{-2\alpha}}{\Gamma^2(1 - \alpha)} + C_3(\alpha, x_0) \frac{t^{-3\alpha}}{\Gamma^3(1 - \alpha)} \quad (51)$$

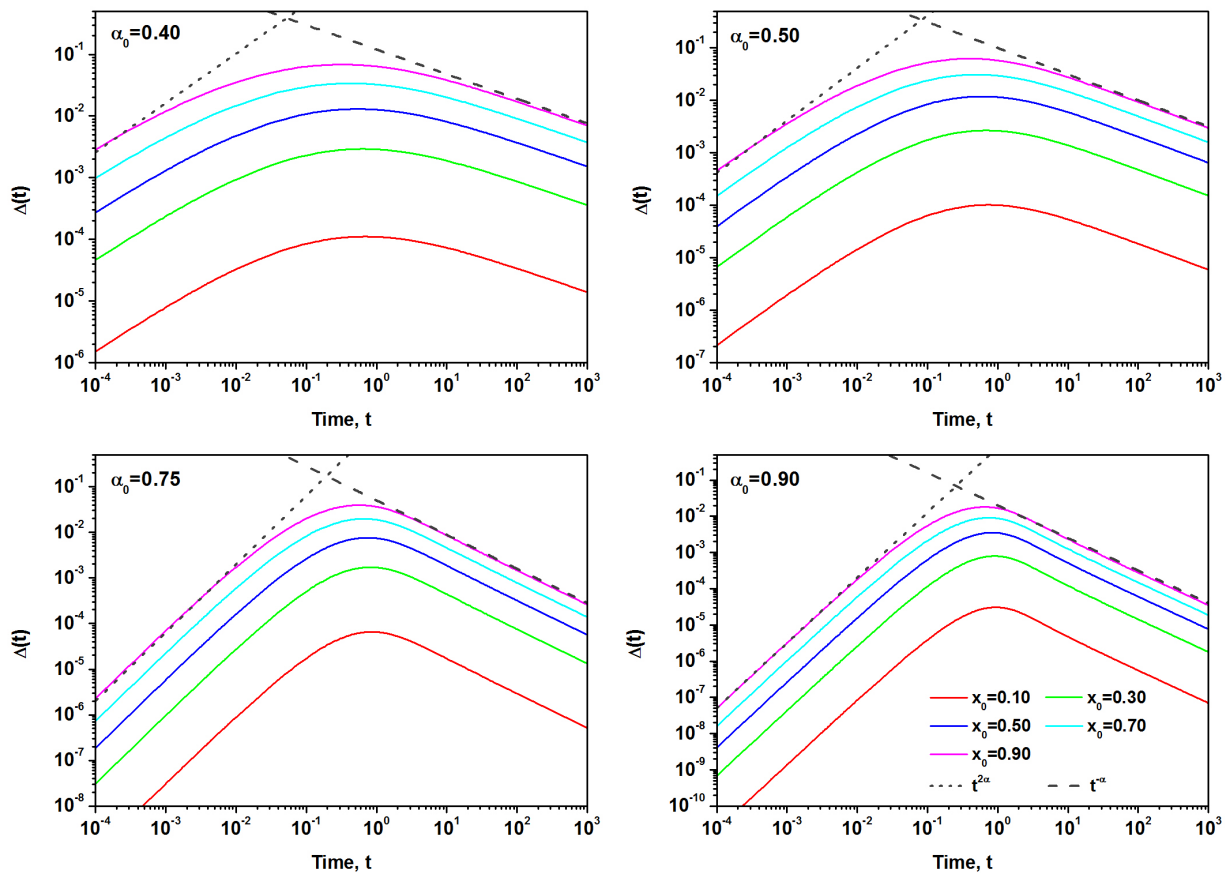


Figure 6. The difference $\Delta(t)$ between the RHS and LHS of the FCE. Consecutive panels correspond to an increasing order of the fractional derivative α . Color lines correspond to range of initial conditions, as denoted by the legend in lower right plot.

130 where C_1, C_2 and C_3 are coefficients depending on α and x_0 , and there is no need to record their values
 131 here.

132 Here again the deviation of the two sides of the FCE using the spectral decomposition analytic solution
 133 and the exact numerical calculation of the fractional derivative results in scaling as depicted in Figure 6.
 134 At early times the deviation increases as $t^{2\alpha}$ whereas at late times the deviation decreases as an inverse
 135 power law in time $t^{-\alpha}$, reaching a maximum at an intermediate time that does not exceed a few percent.

136 7. Numerical solutions

137 Since the analytic solutions to ordinary nonlinear differential equations are notoriously difficult to
 138 find, one turns to numerical methods for assistance. Due to the nonlocal property of the fractional
 139 derivatives, known numerical methods are not easily transferable to the fractional calculus. Herein
 140 we adopted the Adams-Bashforth-Moulton predictor-corrector technique, developed by Diethelm *et al.*
 141 [20,21] to investigate the solutions to fractional Riccati equation, fractional logistic equation and cubic
 142 fractional equation in purely numerical fashion through the numerical integration of the listed equations
 143 The main motivation is to compare the numerical solutions with the ones obtained through spectral
 144 decomposition method.

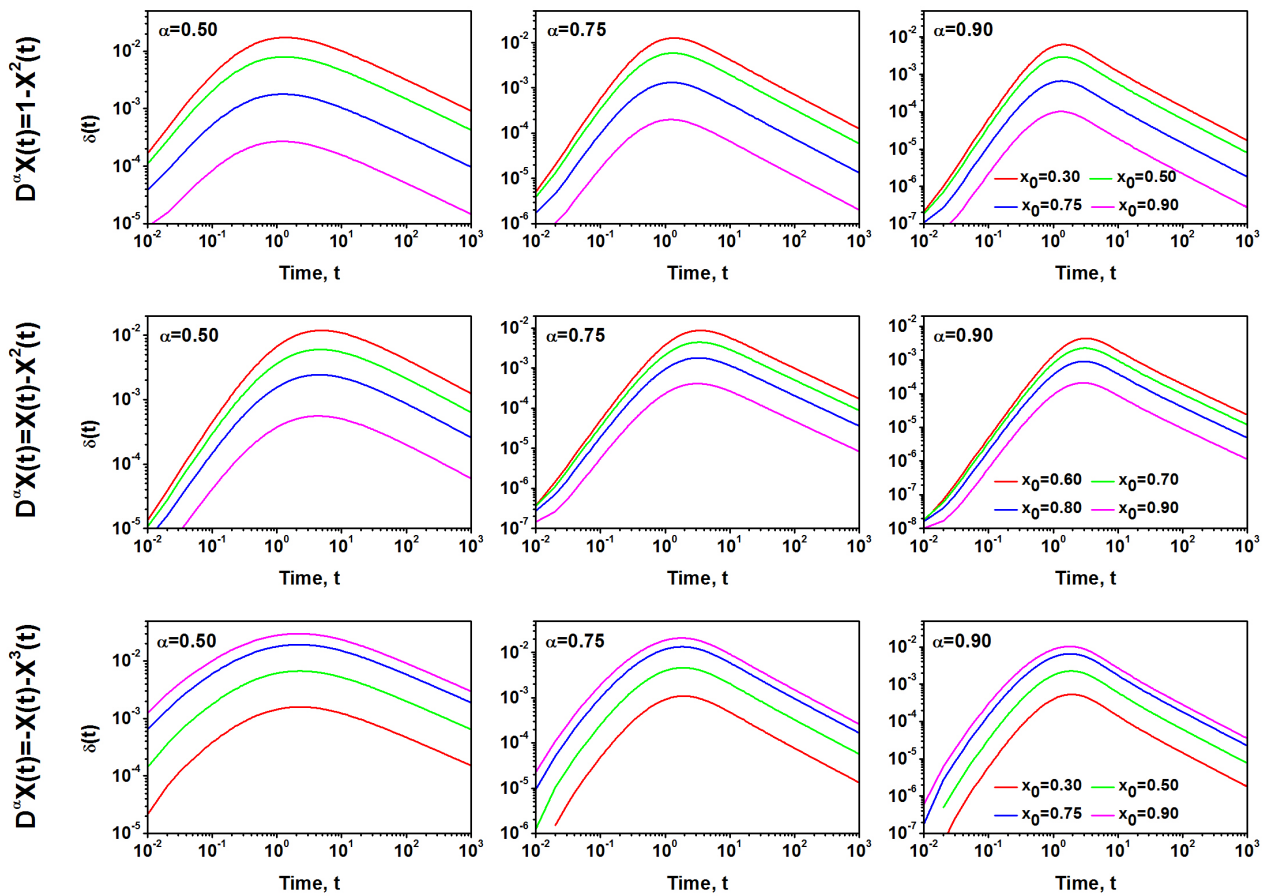


Figure 7. The difference $\delta(t)$ between the numeric integration of fractional differential equations and the solutions obtained with spectral decomposition method.

Solutions for selected values of α and x_0 are presented on Fig. 1, together with the solutions obtained with the spectral decomposition. The overlap of both curves in all cases is extremely good. To better visualize how close the spectral decomposition solution $X_{SP}(t)$ is to the numerical solution $X_{NUM}(t)$, on Figure 7 we plot the difference

$$\delta(t) = X_{NUM}(t) - X_{SP}(t). \quad (52)$$

145 In all cases the difference $\delta(t)$ is smaller than 1% and is characterized by an increase in short time scale,
 146 maximum value at intermediate times and a decrease at large times, where the difference scales as
 147 $t^{-\alpha}$. This result, taken together with the behavior of $\Delta(t)$ demonstrates that the spectral decomposition
 148 method provides analytic solutions that are very close to the true solutions to the fractional nonlinear
 149 differential equations.

150 8. Discussion

151 It has been demonstrated that the spectral decomposition solution to fractional nonlinear dynamic
 152 problems with quadratic and cubic nonlinearities systematically deviate from the evaluation of the
 153 fractional derivative in a common way. The systematic deviation is not monotonic, but for both quadratic
 154 and cubic nonlinearity grows as the same power law at early time, decays as the same inverse power law

155 at late times, and has a maximum deviation of the analytic solution from the numerical evaluation of the
156 fractional derivative of a few percent at some intermediate time. Only the size of the coefficients change
157 with the parameter values and the type of nonlinearity, but not the functional form in time. It appears
158 that the scaling form of the deviation is a consequence of the MLF in the spectral decomposition, which
159 changes as t^α at early times and as $t^{-\alpha}$ at late times.

160 Recall that the FLE was the only other case with which we could compare the solution obtained here
161 with that obtained using a different method and they turned out to be identical. However, the hierarchy
162 of equations solved using the matrix method to solve the FLE [13], implicitly assumed a version of
163 the Leibniz condition. The correspondence of that earlier solution and that obtained using the spectral
164 decomposition method suggests that the deviation from the numerical solution, obtained using the latter
165 technique is related to the Leibniz condition. Unfortunately we have not been able to identify precisely
166 how this comes about and this remains a speculation.

167 Acknowledgments

168 The authors would like to thank the U.S. Army Research Office for supporting this research.

169 Author Contributions

170 MT and BJW conceived and designed the experiments, MT performed the experiments and analyzed
171 the data; MT and BJW wrote the paper.

172 Conflicts of Interest

173 The authors declare no conflict of interest.

174 References

- 175 1. Reyes-Melo, M.E.; Martinez-Vega, J.J.; Guerrero-Salazar, G.A.; Ortiz-Mendez, U. Modeling of
176 relaxation phenomena in organic dielectric materials. Application of differential and integral
177 operators of fractional order. *J Optoelectronics and Adv Mat.* **2004**, *6*, 1037-1043.
- 178 2. Margin, R.L. Fractional calculus models of complex dynamics in biological tissues. *Comps & Math*
179 *with Apps.* **2010**, *59*, 1586-1593. doi: 10.1016/j.camwa.2009.08.039.
- 180 3. Henry, B.I.; Langlands, T.A.M.; Wearne, S.L. Fractional cable models for spiny neuronal dendrites.
181 *Phys Rev Lett.* **2008**, *100*, 128103. doi: <http://dx.doi.org/10.1103/PhysRevLett.100.128103>.
- 182 4. Garra, R. Fractional-calculus model for temperature and pressure waves in fluid-saturated porous
183 rocks. *Phys Rev E.* **2011**, *84*, 036605. doi: <http://dx.doi.org/10.1103/PhysRevE.84.036605>.
- 184 5. Stiassnie, M. On the application of fractional calculus for the formulation of viscoelastic models.
185 *Appl Math Modeling* **1979**, *3*, 300-302. doi: doi:10.1016/S0307 – 904X(79)80063 – 3.
- 186 6. West, B.J. Colloquium: Fractional calculus view of complexity: A tutorial. *Rev Mod Phys.* **2014**,
187 *86*, 1169. doi: <http://dx.doi.org/10.1103/RevModPhys.86.1169>.
- 188 7. West, B.J. *Fractional Calculus View of Complexity. Tomorrow's Science*, 1st ed.; CRC Pub.: Boca
189 Raton, FL, 2015.

- 190 8. Abbasbandy, S. Homotopy perturbation method for quadratic Riccati differential equation and
191 comparison with Adomian's decomposition method. *Appl Meth Comput.* **2006**, *17*, 485-490.
192 doi:10.1016/j.amc.2005.02.014
- 193 9. Khan, N.A.; Ara, A.; Jamil, M. An efficient approach for solving the Riccati equation with fractional
194 orders. *Comput & Math with Appl.* **2011**, *61*, 2683-2680. doi: 10.1016/j.camwa.2011.03.017.
- 195 10. Aminkhah, H.; Hemmatenzhad, M. An efficient method for quadratic Riccati differential equation.
196 *Commun Nonlinear Sci Numer Simul* **2010**, *15*, 835-839. doi:10.1016/j.cnsns.2009.05.009.
- 197 11. Li, Y.; Hu, L. Solving fractional Riccati differential equations using Haar wavelet. In: *Third*
198 *International Conference on Information and Computing*. Wuxi, Jiang Su, China, June 4-6, 2010.
199 doi: 10.1109/ICIC.2010.86.
- 200 12. Svenkeson, A.; Glaz, B.; Stanton, S.; West, B.J. Spectral decomposition of nonlinear systems with
201 memory. unpublished.
- 202 13. West, B.J. Exact solution to fractional logistic equation. *Physica A* **2015**, *429*, 103-108.
203 doi:10.1016/j.physa.2015.02.073.
- 204 14. Zhang, S.; Zong, Q.A.; Liu, D.; Gao, Q. A generalized exp-function method for fractional Riccati
205 differential equations. *Commun Fract Calc.* **2010**, *1*, 48.
- 206 15. West, B.J.; Bologna, M.; Grigolini, P. *Physics of Fractal Operators*, 1st ed.; Springer: New York,
207 2003.
- 208 16. Podlubny, I. *Fractional Differential Equations*, 1st ed.; Academic: New York, 1999.
- 209 17. Davis, H.T. *Introduction to Nonlinear Differential and Integral Equations*, 1st ed.; Dover: New
210 York, 1962.
- 211 18. Jumarie, G. Modified Riemann-Liouville derivative and fractional Taylor series of
212 nondifferentiable functions further results. *Comput & Math with Appl.* **2006**, *51*, 1367-1376.
213 doi:10.1016/j.camwa.2006.02.001
- 214 19. Kowalski, K.; Steeb, W.-H. *Nonlinear Dynamical Systems and Carleman Linearization*, 1st ed.;
215 World Scientific: Singapore, 1991.
- 216 20. Diethelm, K.; Ford, N.J.; Freed, A.D.; Luchko, Y. Algorithms for the fractional calculus: A
217 selection of numerical methods. *Comput Methods Appl Mech Engrg.* **2005**, *194*, 743-773. doi:
218 10.1016/j.cma.2004.06.006.
- 219 21. Diethelm, K.; Ford, N.J.; Freed, A.D. A predictor-corrector approach for the numerical
220 solution of fractional differential equations. *Nonlinear Dynam.* **2002**, *29*, 3-22. doi:
221 10.1023/A:1016592219341.